# **ionocast**: A Real-Time HF/VHF Propagation Prediction Model for Amateur Radio Operators

Toprak Kilic, TA1BUT

April 2026

**Abstract**

**ionocast** provides real-time HF/VHF band-condition verdicts and 3–12 hour forward projections for amateur radio operators. The model runs entirely in the browser with no server-side state; the operator's QTH never leaves the device. It combines an ITU-R P.533–grounded SNR link budget with real-time data from NOAA SWPC (solar indices, D-RAP absorption, OVATION auroral power), the kc2g ionosonde network (observed MUF and foF2), GIRO digisondes (foF2, foEs, hmF2), and WSPR spot observations from `wspr.live`. A 70/30 ensemble blend with an N0NBH-style SFI heuristic anchors predictions to community-calibrated expectations, while a local validation harness corrects systematic bias via per-group, per-horizon offsets derived from retrospective WSPR scoring. Key contributions include an *asymmetric MUF consensus* that trusts observations over climatology when the ionosphere is declining, a *power-summed noise model* that correctly handles man-made noise dominance on the low bands, *per-hop minimum MUF* via great-circle ray geometry, *elevation-dependent antenna gain* from hop-geometry-derived takeoff angles, *NVIS detection* for short paths using foF2, and *Dst/IMF Bz integration* for earlier storm detection than Kp alone. Both short-path and long-path great circles are evaluated per destination. All computation is deterministic, repeatable, and inspectable; no machine-learning black boxes.

## Contents

# 1 Introduction

Amateur radio operators planning an operating session need to answer a deceptively simple question: *which bands will be open, and for how long?* The answer depends on the instantaneous state of the ionosphere, the Sun, the geomagnetic field, and the operator's own station (antenna, power, mode, and local noise environment).

Existing tools serve fragments of this problem:

- **VOACAP** [1] provides rigorous P.533-based predictions but operates as a batch tool requiring manual circuit specification; it is not real-time.
- **N0NBH Solar Conditions** provides a widely trusted heuristic band-condition table keyed to SFI and Kp, but without path geometry or operator context.
- **kc2g MUF map** renders observed MUF contours in near real time, but offers no forward projection and no SNR context.
- **HamQSL / DX Toolbox** use threshold-based rules on solar indices, lacking physics grounding.

**ionocast** occupies the intersection: real-time, physics-grounded, operator-configurable, and privacy-preserving. The operator's QTH (stored in `localStorage` only) parameterises five reference propagation paths; the SNR budget runs per band, per path, per time-step. Forward projections at +3, +6, +9, and +12 hours use solar-zenith analogy, storm depression, seasonal correction, and sporadic-E persistence.

This paper documents the complete model as implemented, with every numeric constant, so that the amateur radio community can audit, reproduce, and improve it.

# 2 Data Sources

Table 1 lists all upstream data feeds. Sources marked "Direct CORS" are fetched by the browser with no server proxy; sources marked "Proxied" pass through a Cloudflare Worker endpoint that resolves the operator's Maidenhead grid to a station identifier server-side.

Table 1: Upstream data sources and refresh cadences.

| Source | Data | Refresh | Protocol |
|---|---|---|---|
| NOAA SWPC | Kp, Ap, F10.7, X-ray class, 3-day forecast, 27-day outlook, D-RAP HAF, OVATION aurora HP, solar-wind Bz/speed/density, solar regions | 1–10 min | Direct CORS JSON/text |
| prop.kc2g.com | Per-station MUF(3000F2), foF2, TEC | ∼15 min | Direct CORS JSON |
| GIRO (lgdc.uml.edu) | Nearest digisonde foF2, foEs, hmF2 | ∼10 min | Proxied via `/api/giro` |
| GFZ Potsdam | Hp30 nowcast | 30 min | Proxied via `/api/hp30` |
| WDC Kyoto | Dst / Sym-H | 1 h | Proxied via `/api/kyoto` |
| SILSO | Daily sunspot number | Daily | Proxied via `/api/silso` |
| UWyo | Radiosonde soundings ($\Delta N$ for tropospheric ducting) | 12 h | Proxied via `/api/tropo` |
| wspr.live | WSPR spot counts and SNR by band | 10 min | Direct CORS (ClickHouse) |
| NASA DONKI | CME and HSS analyses | ∼hours | Direct CORS JSON |

## 2.1 Privacy Model

The operator's QTH is stored exclusively in `localStorage` and never transmitted to any ionocast server. WSPR queries use only the two-character Maidenhead field (an ∼18°×20° rectangle),

providing geographic context without meaningful localisation. Proxied endpoints (`/api/giro`, etc.) resolve the QTH to the nearest station code server-side; the response contains only station data, not the query coordinates.

**First-visit default.** On first load, with no saved QTH, ionocast derives a regionally plausible grid from the browser's runtime timezone. `Intl.DateTimeFormat().resolvedOptions().timeZone` is looked up in a compiled table of ∼60 major ham-active IANA zones (e.g. `Europe/Berlin` → JO62, `Asia/Tokyo` → PM95, `Australia/Sydney` → QF56). Zones outside the table synthesise a grid from the UTC offset: longitude ≈ offset × 15° at a fixed mid-latitude (45° N for the northern hemisphere, −35° for identified southern-hemisphere zones). The timezone fingerprint is already exposed on every HTTPS request, so using it for a first-visit default adds no new privacy surface. When even that math fails, the last-resort fallback is **JN05** (45° N, 0° E) — the ITU-R canonical mid-latitude reference point where the CCIR R-12 / P.1239 foF2 coefficients underlying this paper are tabulated. No request is ever made to a geolocation service.

# 3 SNR Budget Model

The core of ionocast is a complete link budget that computes the SNR margin $M$ (in dB) for each amateur band on each reference path:

$$M = P_{\text{tx}} + G_{\text{ant}} - L_{\text{fs}} - L_{\text{abs}} - L_{\text{absD}} - L_{\text{aur}} - L_{\text{MUF}} - L_{\text{iono}} - L_{\text{low}} - L_{\text{hop}} - L_{\text{Es}} - N - S_{\text{req}} \quad (1)$$

where every term is defined in the following subsections. A positive $M$ means the signal exceeds the minimum required SNR for the chosen mode; the magnitude indicates robustness.

## 3.1 Free-Space Loss (Friis / ITU-R P.525)

$$L_{\text{fs}} = 32.44 + 20\log_{10}(d_{\text{km}}) + 20\log_{10}(f_{\text{MHz}}) \quad (2)$$

The distance $d_{\text{km}}$ is the great-circle path length, clamped to a minimum of 50 km to avoid numerical singularity on extremely short paths.

## 3.2 MUF Approach and Over-MUF Loss (ITU-R P.533 §3.2.2)

Let $r = f/\text{MUF}$. The proximity loss is:

$$L_{\text{MUF}} = \begin{cases} 0 & r \le 0.70 \\ 10\left(\dfrac{r - 0.70}{0.30}\right)^2 & 0.70 < r \le 1.00 \\ 10 + 36\sqrt{r - 1} & r > 1.00 \end{cases} \quad (3)$$

Below 70% of MUF the ionosphere provides comfortable refraction with negligible loss. Between 70–100% the loss rises quadratically. Above MUF (over-MUF operation, e.g. via Es or scatter), the loss escalates rapidly.

## 3.3 D-Region Absorption: Flare-Enhanced (SWPC D-RAP)

SWPC's D-RAP product provides a Highest Affected Frequency (HAF) in MHz. The flare-enhanced absorption is:

$$L_{\text{abs}} = \begin{cases} 0 & \text{HAF}/f < 0.3 \\ 3\left(\dfrac{\text{HAF}}{f}\right)^{1.5} & \text{otherwise} \end{cases} \quad (4)$$

### 3.4 D-Region Absorption: Quiet-Day Diurnal (ITU-R P.533 §4)

$$L_{\text{absD}} = A_{\text{base}}(f) \cdot (\cos\chi)^{1.3} \tag{5}$$

where $\chi$ is the solar zenith angle at the path midpoint. At night ($\cos\chi < 0.05$), $L_{\text{absD}} = 0$. The base absorption values follow K9LA quiet-day estimates (Table 2).

Table 2: Quiet-day D-region base absorption $A_{\text{base}}$ by band.

| **Band** | $A_{\text{base}}$ (dB) |
|---|---|
| 160 m | 28 |
| 80 m | 18 |
| 60 m | 10 |
| 40 m | 6 |
| 30 m | 2 |
| 20 m | 0.5 |
| 15 m+ | 0 |

### 3.5 Auroral Absorption (CGM-Gated)

Auroral absorption activates only when the corrected geomagnetic (CGM) latitude of the path midpoint satisfies $|\phi_{\text{CGM}}| \geq 60°$:

$$L_{\text{aur}} = \min\left(30,\ D \cdot \frac{30}{f_{\text{MHz}}}\right) \tag{6}$$

where

$$D = \max\left(5(K_p - 4),\ \frac{\text{HP}_{\text{GW}} - 50}{5}\right) \tag{7}$$

when either $K_p \geq 5$ or the OVATION hemispheric power HP $\geq 50$ GW.

The CGM latitude is computed via a tilted-dipole approximation:

$$\phi_{\text{CGM}} = \arcsin\big(\sin\phi \sin\phi_P + \cos\phi \cos\phi_P \cos(\lambda - \lambda_P)\big) \tag{8}$$

with the IGRF 2020 north magnetic pole at $\phi_P = 80.7°$N, $\lambda_P = 72.7°$W.

### 3.6 Multi-Hop Ground Reflection Loss

Each ground reflection costs 5 dB:

$$L_{\text{hop}} = 5\,(N_{\text{hops}} - 1) \quad \text{dB}, \qquad N_{\text{hops}} = \lceil d_{\text{km}}/4000 \rceil \tag{9}$$

### 3.7 Sporadic-E Screening Loss

When a strong Es layer is present ($f_{\text{oEs}} \geq 5$ MHz) and the operating frequency is below twice the Es critical frequency ($f < 2\,f_{\text{oEs}}$), the layer partially screens the F2 reflection:

$$L_{\text{Es}} = 5\,\text{dB} \tag{10}$$

### 3.8 Low-Band Extra Loss

A step-function accounts for additional empirical losses on the lower HF bands (ground-wave coupling, higher-angle refraction, congestion):

| **Band** | $L_{\text{low}}$ (dB) |
|---|---|
| 160 m | 8 |
| 80 m | 5 |
| 60 m | 3 |
| 40 m | 2 |
| 30 m+ | 0 |

### 3.9 Lumped Ionospheric Loss

$$L_{\text{iono}} = 15\,\text{dB} \tag{11}$$

This lumps three P.533 terms that are not individually modelled: spatial focusing/defocusing $L_z \approx 3\,\text{dB}$, above-median variability plus polarisation coupling $Y_p \approx 9\,\text{dB}$, and residual terms $\approx$3 dB. It does *not* include D-region absorption (handled by $L_{\text{absD}}$ and $L_{\text{abs}}$) or ground reflection (handled by $L_{\text{hop}}$).

### 3.10 Noise Model (ITU-R P.372)

The received noise power is computed as a *power sum* of atmospheric and man-made components, ensuring the total never drops below the galactic/man-made floor:

$$N = 10\log_{10}\left(10^{N_{\text{atmo}}/10} + 10^{N_{\text{mm}}/10}\right) \tag{12}$$

where:

$$N_{\text{atmo}} = N_{\text{base}}(f) + \Delta N_{\text{diurnal}}(f, \cos\chi) \tag{13}$$

$$N_{\text{mm}} = N_{\text{base}}(f) + F_a \tag{14}$$

The diurnal swing is:

$$\Delta N_{\text{diurnal}} = -A \cdot \text{clamp}(\cos\chi,\, -1,\, 1) \tag{15}$$

with $A = 10\,\text{dB}$ for $f \leq 10\,\text{MHz}$ and $A = 3\,\text{dB}$ above. The man-made noise factor $F_a$ depends on environment: rural 0 dB, suburban +15 dB, urban +25 dB.

Table 3 gives the baseline noise power at 2.5 kHz reference bandwidth.

Table 3: Baseline noise $N_{\text{base}}$ from ITU-R P.372 at 2.5 kHz bandwidth.

| **Band** | $N_{\text{base}}$ (dBm) |
|---|---|
| 160 m | -110 |
| 80 m | -115 |
| 60 m | -118 |
| 40 m | -122 |
| 30 m | -125 |
| 20 m | -128 |
| 17 m | -131 |
| 15 m | -132 |
| 12 m | -133 |
| 10 m | -134 |

### 3.11 Required SNR by Mode

| **Mode** | $S_{\text{req}}$ (dB) |
|---|---|
| SSB | +10 |
| CW | +3 |
| FT8 | -21 |
| FT4 | -13 |
| WSPR | -25 |

### 3.12 Antenna Elevation Pattern

The antenna gain $G_{\text{ant}}$ is not a flat scalar; it varies with the required takeoff (elevation) angle. The elevation is derived from hop geometry using a simplified flat-earth model:

$$\theta_{\text{elev}} = \arctan\left(\frac{2\,h_F}{d_{\text{hop}}}\right) \tag{16}$$

where $h_F = 300\,\text{km}$ (typical F2 height) and $d_{\text{hop}} = d/N_{\text{hops}}$. Long-haul DX paths require low takeoff angles (5–10°); regional paths use higher angles (15–30°); NVIS uses near-vertical (60–90°).

Each antenna type has a characteristic elevation response:

- **Dipole at 10 m** (+5 dBi peak): deep null below 8° (−10 dB), peak at 15–60°. Poor for DX, good for regional/NVIS.
- **Vertical** (+2 dBi peak): best at low angles (5–25°), drops off above 25°. Good for DX, poor for NVIS.
- **Yagi** (+9 dBi+ peak): focused, excellent low-angle gain. Best for DX; falls off sharply above the main lobe.
- **Indoor/compromise** ($\leq 0$ dBi): nearly omnidirectional, small low-angle penalty from ground proximity.

The effective gain at the required elevation replaces the flat peak-gain scalar in the SNR budget, making verdicts genuinely personal to the operator's antenna type and the path geometry.

### 3.13 Default Operator Settings

The default station profile assumes a typical amateur installation: $P_{\text{tx}} = 50\,\text{dBm}$ (100 W), $G_{\text{ant}} = +5\,\text{dBi}$ peak (installed dipole with ground reflection; effective gain varies by path elevation), mode = SSB, noise environment = suburban.

### 3.14 Worked Example: 20 m, 3000 km, Quiet Day

Figure 1 illustrates the complete budget for a 14.1 MHz path of 3000 km on a quiet day.

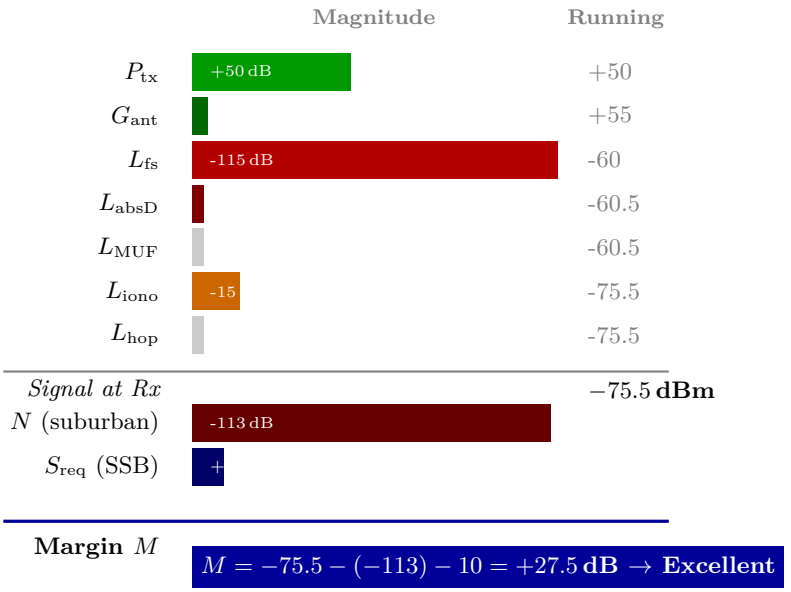


Figure 1: SNR budget waterfall for 20 m (14.1 MHz), 3000 km, quiet day, suburban noise, SSB. The 27.5 dB margin corresponds to an "Excellent" verdict.

# 4 MUF Estimation

The Maximum Usable Frequency is the single most important input to the link budget. ionocast derives it from three sources in a consensus blend.

## 4.1 kc2g Observed MUF

The kc2g network publishes MUF(3000F2) from each ionosonde. For each of five reference paths (midpoints near New York, São Paulo, Johannesburg, Tokyo, Sydney), ionocast selects the nearest ionosonde. A *freshness gate* discards observations older than 30 min. The distance from each path midpoint to its nearest ionosonde is displayed in the path table so operators can gauge data confidence; stations beyond 1500 km are flagged.

## 4.2 foF2 Climatology (Simplified P.1239)

When observed data are stale or unavailable, ionocast falls back to a simplified climatological model:

$$f_{\mathrm{oF2}} = \max\bigl(2,\ (3.5 + 0.04(F_{10.7\mathrm{A}} - 70)) + 4.0(1 - 0.003|\phi|) \cdot \max(0, \cos\chi)\bigr) \tag{17}$$

with $\mathrm{MUF}(3000) \approx 3.0 \times f_{\mathrm{oF2}}$.

## 4.3 Asymmetric Consensus Blend

The consensus algorithm treats upward and downward divergence differently, reflecting the physical asymmetry that a declining ionosphere (afternoon/evening) is far more common than spurious low station readings:

1. Compute divergence: $\delta = |\ln(\mathrm{MUF}_{\mathrm{kc2g}}/\mathrm{MUF}_{\mathrm{climo}})|$
2. If $\delta \leq \ln 1.5$: use the geometric mean $\sqrt{\mathrm{MUF}_{\mathrm{kc2g}} \cdot \mathrm{MUF}_{\mathrm{climo}}}$
3. If kc2g < climatology (declining ionosphere): **trust kc2g**
4. If kc2g > climatology (possible station anomaly): **fall to climatology**

### 4.4 Per-Hop Minimum MUF (P.533 §3.1)

For paths requiring $N \geq 2$ hops, each reflection point at fraction $(2k-1)/(2N)$ along the great circle may see a different solar illumination. The path MUF is the *minimum* across all hops:

$$\mathrm{MUF}_{\mathrm{path}} = \min_{k=1}^{N} \mathrm{MUF}_{\mathrm{mid}} \cdot \frac{S(\cos\chi_k,\, F)}{S(\cos\chi_{\mathrm{mid}},\, F)} \tag{18}$$

where $S(c, F) = \max\bigl(F,\, \sqrt{\max(0.05,\, c)}\bigr)$ is the zenith-shape function and $F$ is the night floor.

### 4.5 Night Floor (CCIR/IRI)

The night floor scales with solar activity and latitude:

$$F = \mathrm{clamp}\left(0.25 + 0.0025(F_{10.7\mathrm{A}} - 70) - 0.10\,\min\left(1,\, \frac{|\phi|}{60}\right),\, 0.20,\, 0.60\right) \tag{19}$$

### 4.6 NVIS Detection for Short Paths

For paths shorter than 500 km on bands at or below 8 MHz (160 m through 40 m), the signal travels at near-vertical incidence (NVIS). The relevant frequency limit is the *critical frequency* $f_{\mathrm{oF2}}$ (vertical reflection), not MUF(3000) (oblique reflection at ∼3000 km range). Since $\mathrm{MUF}(3000) \approx 3 \times f_{\mathrm{oF2}}$, using MUF(3000) for short paths over-predicts by up to a factor of three.

When a short NVIS path is detected, ionocast automatically substitutes the GIRO-observed $f_{\mathrm{oF2}}$ from the nearest digisonde as the effective MUF. No operator action is required.

### 4.7 Short-Path vs. Long-Path Evaluation

Between any two points on Earth there are two great-circle paths. The long path (LP) traverses the opposite side of the globe and can be open when the short path (SP) is closed, particularly at dawn and dusk on 20 m and 17 m.

For each of the five reference destinations, ionocast computes both the SP and LP midpoints, finds the nearest kc2g ionosonde for each, and evaluates margins on both paths. The LP midpoint is the antipode of the SP midpoint: $(-\phi_{\mathrm{mid}},\, \lambda_{\mathrm{mid}} + 180°)$. Both paths compete for the best-margin verdict, so an open LP beats a closed SP whenever it offers a better budget.

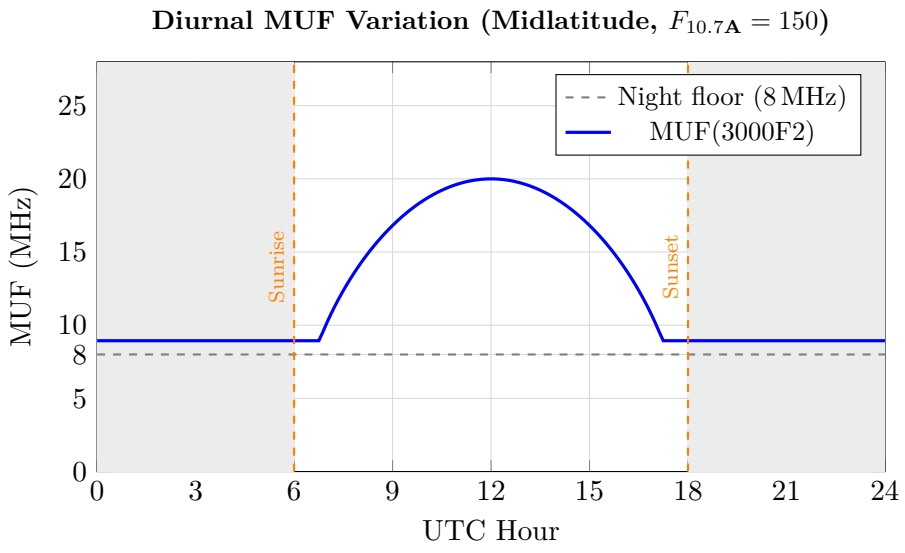


Figure 2: Diurnal MUF variation showing the $\sqrt{\cos\chi}$ shape scaled to a peak of 20 MHz with night floor at 8 MHz (shaded regions = night).

# 5 Forward Projection (3–12 h)

The forward projection engine extends the current nowcast into the future by modelling the dominant drivers of ionospheric change.

## 5.1 MUF Projection via Solar Zenith Analogy

$$\mathrm{MUF}_{\mathrm{future}} = \mathrm{MUF}_{\mathrm{now}} \cdot \frac{S(\cos\chi_{\mathrm{future}},\, F)}{S(\cos\chi_{\mathrm{now}},\, F)} \cdot R_{\mathrm{seasonal}} \cdot F_{\mathrm{storm}} \tag{20}$$

## 5.2 Seasonal Ratio

$$R_{\mathrm{seasonal}} = \frac{s(t_{\mathrm{future}},\, \phi)}{s(t_{\mathrm{now}},\, \phi)} \tag{21}$$

where

$$s(t, \phi) = 1 + (0.15\cos\theta + 0.08\cos(2\theta + \pi)) \cdot w(\phi) \tag{22}$$

with $\theta = (m - 1 - h \cdot 6) \cdot 2\pi/12$, $h$ being the hemisphere flag (+1 north, −1 south), and $w(\phi) = \min(1, |\phi|/50)$. The first term captures the annual winter-peak/summer-trough at midlatitudes; the second captures the semi-annual equinox peaks (March, September) evident in F2-layer statistics.

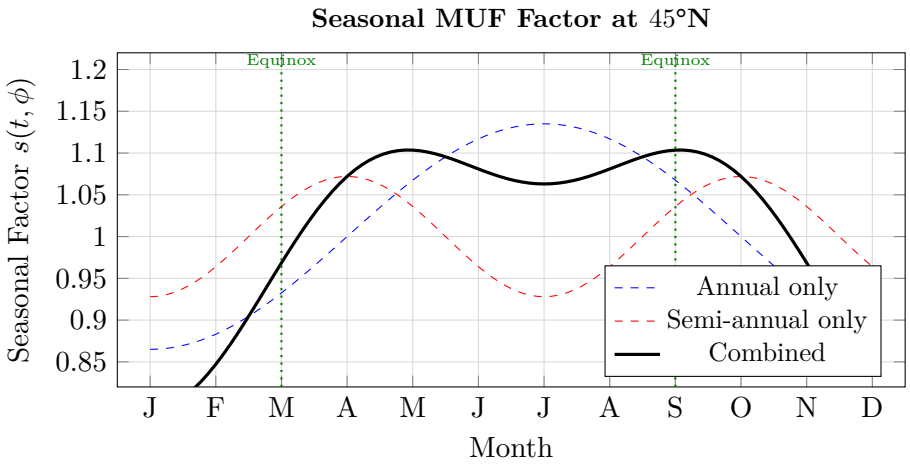


Figure 3: Seasonal MUF factor at 45°N showing annual (winter peak) and semi-annual (equinox peaks) components.

## 5.3 Storm Depression

When $K_p > 4$, the MUF is depressed:

$$F_{\mathrm{storm}} = \max(0.5,\ 1 - p\,(K_p - 4)) \tag{23}$$

where

$$p = 0.05 + 0.10 \cdot \mathrm{clamp}\left(\frac{|\phi_{\mathrm{CGM}}| - 40}{30},\ 0,\ 1\right) \tag{24}$$

At midlatitudes ($|\phi_{\mathrm{CGM}}| = 40°$), the damping is 5% per $K_p$ unit above 4. In the auroral zone ($|\phi_{\mathrm{CGM}}| = 70°$), it rises to ∼15% per unit.

### 5.3.1 Dst and IMF Bz as Secondary Storm Drivers

The 3-hour Kp index is a lagging indicator. Two faster-responding indices are wired into the storm model:

- **Dst** (Kyoto ring-current index): when Dst $< -50$ nT, the effective $K_p$ is bumped by up to $+2$ (1 per 50 nT below $-50$). Dst responds within minutes of storm onset, 1–3 hours before Kp updates.
- **IMF Bz** (DSCOVR L1 solar wind): sustained southward Bz ($< -5$ nT) predicts substorm onset within 1–3 hours. The near-term ($\leq 6$ h) Kp forecast is boosted by $+1.5$ when Bz is southward.

Both adjustments are capped at $K_p = 9$ and apply only when the respective index is available. During severe storms ($K_p \geq 7$), the auroral absorption CGM threshold also expands from 60° to 50° to capture the equatorward expansion of the auroral oval.

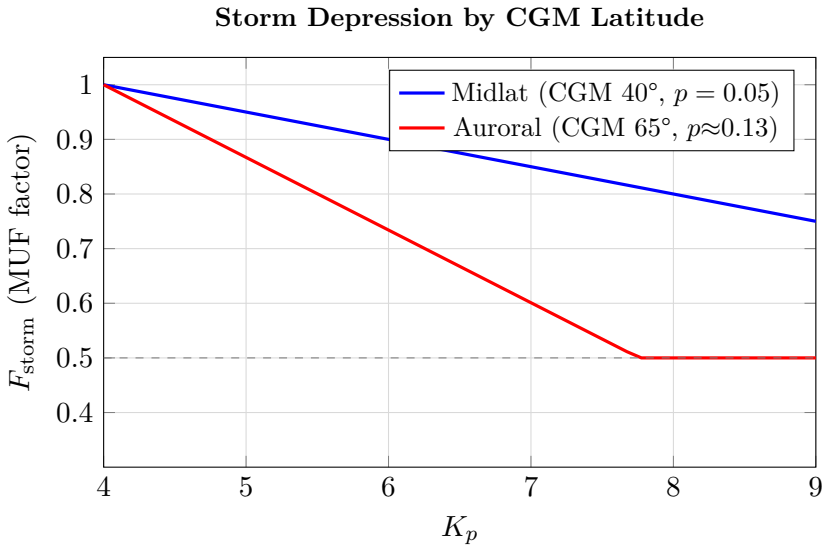


Figure 4: Storm MUF depression factor vs. $K_p$ for midlatitude and auroral-zone paths. The floor is clamped at 0.5 (50% depression).

## 5.4 Sporadic-E Persistence

The projected critical frequency of the sporadic-E layer decays exponentially:

$$f_{\mathrm{oEs}}(t + \Delta) = \max\Big(B,\ f_{\mathrm{oEs}}(t) \cdot 2^{-\Delta/\tau}\Big) \tag{25}$$

with half-life $\tau = 1.5$ h at night, 3.0 h during the day. The background $B = 2$ MHz when $\cos\chi > 0.2$, otherwise 0.

## 5.5 Gray-Line Bonus

When the reflection midpoint lies near the solar terminator ($|\cos\chi| < 0.1$) the D-region is thin, so a small additive bonus is applied to the margin. The effect is strongest on the low bands — where D-region absorption normally dominates the budget — and fades away by the upper HF. The bonus is

$$B_{\mathrm{GL}}(f) = \begin{cases} 5\,\mathrm{dB} \cdot p & f \leq 4\,\mathrm{MHz} \quad (160, 80\,\mathrm{m}) \\ 4\,\mathrm{dB} \cdot p & 4 < f \leq 8\,\mathrm{MHz} \quad (60, 40\,\mathrm{m}) \\ 2\,\mathrm{dB} \cdot p & 8 < f \leq 11\,\mathrm{MHz} \quad (30\,\mathrm{m}) \\ 1\,\mathrm{dB} \cdot p & 11 < f \leq 14\,\mathrm{MHz} \quad (20\,\mathrm{m}) \\ 0 & f > 14\,\mathrm{MHz} \end{cases} \tag{26}$$

with proximity $p = 1 - \min(1, |\cos\chi|/0.1)$ so the bonus scales linearly from zero at $|\cos\chi| = 0.1$ to full amplitude at the terminator itself. Above 14 MHz the D-region already contributes little to the path budget, so no bonus is modelled.

# 6 Ensemble Blend and Self-Calibration

## 6.1 Blended Margin

The final margin is a weighted average of the physics-based model and a community-calibrated heuristic:

$$M_{\text{blend}} = 0.7\,(M_{\text{physics}} + B_{g,\Delta h}) + 0.3\,M_{\text{heuristic}} \tag{27}$$

## 6.2 N0NBH-Style Heuristic

The heuristic encodes per-band rules derived from N0NBH's SFI/Kp-based band condition conventions. Each band has its own rule set reflecting its propagation character (e.g. 160 m is night-only; 30 m works all day; 10 m needs high SFI). The returned tier maps to a dB equivalent:

| **Heuristic Tier** | $M_{\text{heuristic}}$ (dB) |
|---|---|
| Excellent | +20 |
| Good | +10 |
| Fair | 0 |
| Poor | -10 |
| Closed | -18 |

## 6.3 Bias Correction from Validation Harness

The self-calibration harness (Section 6) accumulates retrospective scoring against WSPR observations. The bias correction per band $g$ and forecast horizon $\Delta h$ is:

$$B_{g,\Delta h} = 11 \cdot \overline{(r_{\text{actual}} - r_{\text{predicted}})} \quad \text{dB} \tag{28}$$

where $r$ denotes the tier index (Excellent=4, …, Closed=0) and the factor 11 converts tier-units to dB using the constant tier width. The correction activates only when $n \geq 10$ scored samples exist; below threshold, $B = 0$.

## 6.4 Tier Probabilities

Given the blended margin $M$ and spread $\sigma$, the probability of achieving at least tier $T$ is:

$$P(\text{tier} \geq T) = 1 - \Phi\left(\frac{\theta_T - M}{\sigma}\right) \tag{29}$$

where $\Phi$ is the standard normal CDF and $\theta_T$ is the tier threshold (Table 4).

The spread $\sigma$ is *condition-dependent*, computed as the RSS of a base uncertainty (8 dB, ITU-R P.533 range 6–10 dB) and three situational penalties:

- **Near-MUF:** when $f/\text{MUF} > 0.85$, fading and multipath intensify. Adds up to +4 dB at $f = \text{MUF}$.
- **Storm:** $K_p \geq 5$ produces ionospheric irregularities. Adds +3 dB at $K_p = 5$, scaling to +6 dB at $K_p = 9$.
- **Cross-terminator:** when the path midpoint has $|\cos\chi| < 0.15$ (sunrise/sunset line), sharp electron-density gradients increase variance by +3 dB.

All penalties are added in quadrature: $\sigma = \sqrt{8^2 + \sigma_{\text{MUF}}^2 + \sigma_{\text{storm}}^2 + \sigma_{\text{term}}^2}$.

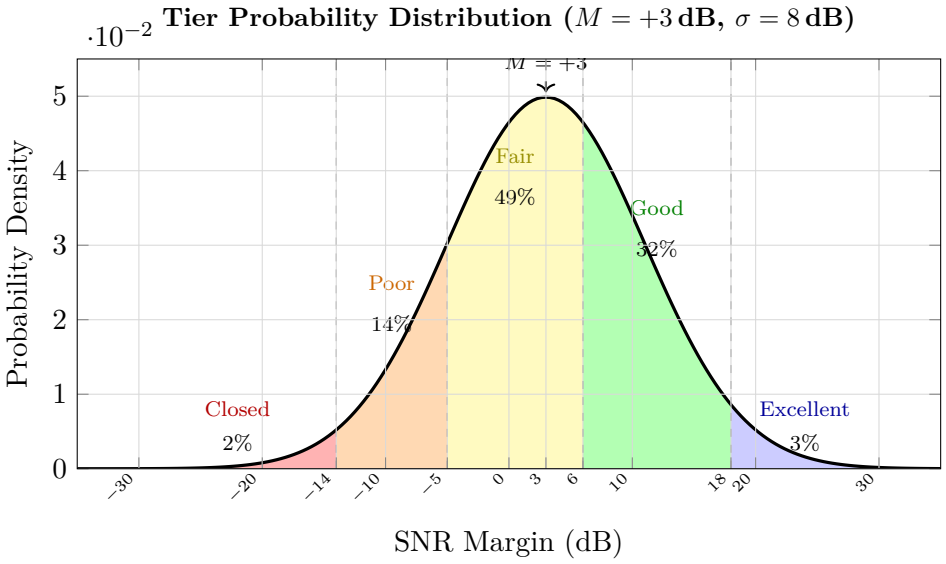


Figure 5: Tier probability distribution for a blended margin of +3 dB with $\sigma = 8$ dB. The most likely tier is Fair (49%), with a 35% chance of Good or better.

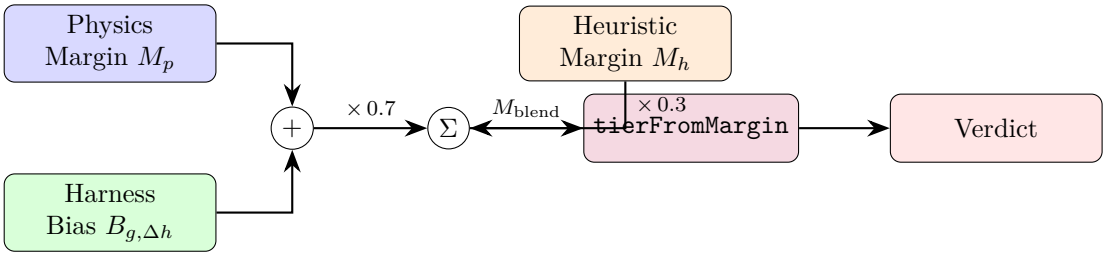


Figure 6: Ensemble blend flow diagram. The physics margin (with harness bias correction) receives 70% weight; the N0NBH-style heuristic receives 30%.

## 7 Tier Mapping

Verdicts are computed *per band* (160 m through 10 m individually, plus 6 m and 2 m for VHF), not in groups. For each band the SNR margin is evaluated on every reference path (short and long, across all five destinations); the **best-margin** path wins and its margin drives the verdict, while the reason string and `openDirs` list record which destination that was. If a single path is viable, the band is not "closed" — it is open to that destination, which is material information for the operator. An earlier aggregation over the median margin was removed because most reference paths are long transcontinental hops that are routinely over-MUF or night-crossing; the median was dominated by failing paths and buried genuinely open short paths (e.g. a 944 km EM79–NYC path reporting +27 dB margin would have its verdict overwritten by the median of eight failing long paths).

The continuous margin is discretised into five operator-facing tiers (Table 4).

Table 4: Tier thresholds.

| **Tier** | Margin Threshold (dB) | **Meaning** |
|---|---|---|
| Excellent | $\geq +18$ | Signals well above noise; reliable copy |
| Good | $\geq +6$ | Comfortable contacts expected |
| Fair | $\geq -5$ | Marginal; digital modes work, SSB intermittent |
| Poor | $\geq -14$ | Weak/absent signals; only FT8/WSPR viable |
| Closed | $< -14$ | Band effectively closed |

### 7.1 WSPR Spot-Reality Override

When WSPR spot counts for a band clearly exceed the band's typical busy-hour baseline but the physics tier is Poor or Closed, the verdict is bumped to Fair. When the excess is extreme (five times the threshold or more) the bump goes all the way to Good. Conversely, when the physics tier is Excellent or Good but spot counts are well below baseline (less than 10 % of threshold), the verdict is downgraded one tier. The override is a bidirectional sanity check, not a one-way promotion.

**Data-driven baselines.** Thresholds are indexed by (band, UTC-hour) rather than by a flat per-band constant. The calibration pipeline (`scripts/calibrate-wspr.mjs`) issues a single ClickHouse query against the wspr.live mirror:

```
SELECT band, toHour(time) AS hour_utc,
       quantile(0.75)(hourly_count) AS p75
FROM (
 SELECT band, toStartOfHour(time) AS h,
        toHour(time) AS hour_utc,
        count() AS hourly_count
 FROM wspr.rx
 WHERE time >= now() - INTERVAL 30 DAY
       AND toDayOfWeek(time) < 6
 GROUP BY band, h, hour_utc
) GROUP BY band, hour_utc
```

This produces a $10 \times 24$ matrix of hourly spot rates, one per band per UTC hour, using the 75th percentile across 30 days of data with weekends excluded (cheap proxy for contest-weekend filtering). The override threshold is $T_{\text{spot}}(b, h) = \max(50,\ 1.5 \cdot p_{75}(b, h))$, so ordinary busy-hour activity (the top quartile of weekday hours) sits just below the threshold, and the override fires only on activity that is anomalously high for that band-hour cell.

The baseline matrix is emitted as a plain ES module at `src/spot-baselines.mjs` and imported at runtime by the derive pipeline. It should be re-generated every few months or any time band-activity patterns drift (solar-cycle phase, major geomagnetic events), and is versioned with the rest of the codebase so fresh checkouts ship with valid baselines out of the box.

**Sensitivity.** Both knobs in the calibration script are tunable:

- `THRESHOLD_MULTIPLIER` (default 1.5) scales the percentile. Lower it to fire the override more aggressively (set to 1.0 for "fires when at or above p75"); raise it to reserve the override for very anomalous openings.
- The percentile itself (default p75) can be swapped for p50 (median-active) or p90 (only clearly exceptional hours) with a one-line edit.

Because the baselines encode the diurnal pattern directly, no separate day/night multiplier is needed; the hourly resolution is finer than the sinusoidal model it replaces.

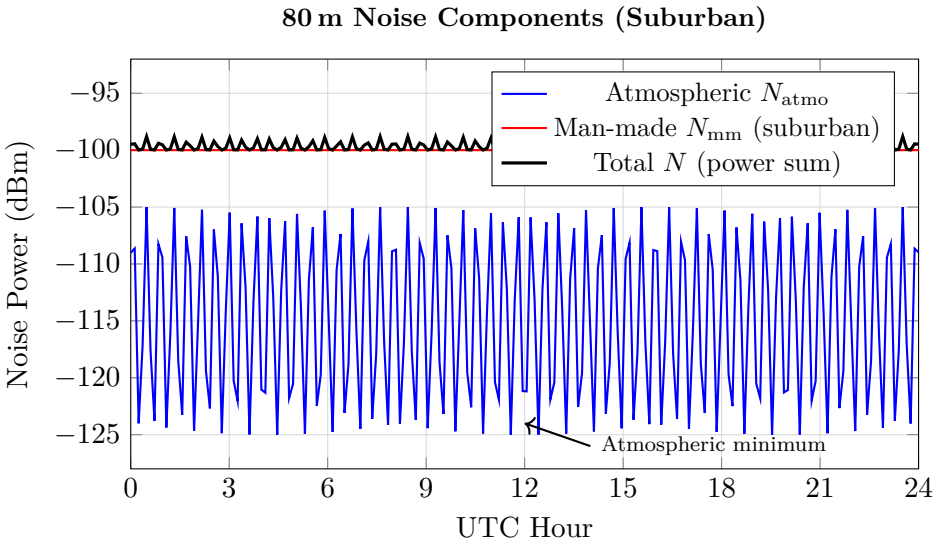


Figure 7: Noise power components on 80 m in a suburban environment. The man-made noise (-100 dBm) dominates at all hours; the atmospheric diurnal swing barely affects the total. This power-sum model prevents the phantom 7 dB margin that a linear (dB-domain) sum would produce at midday.

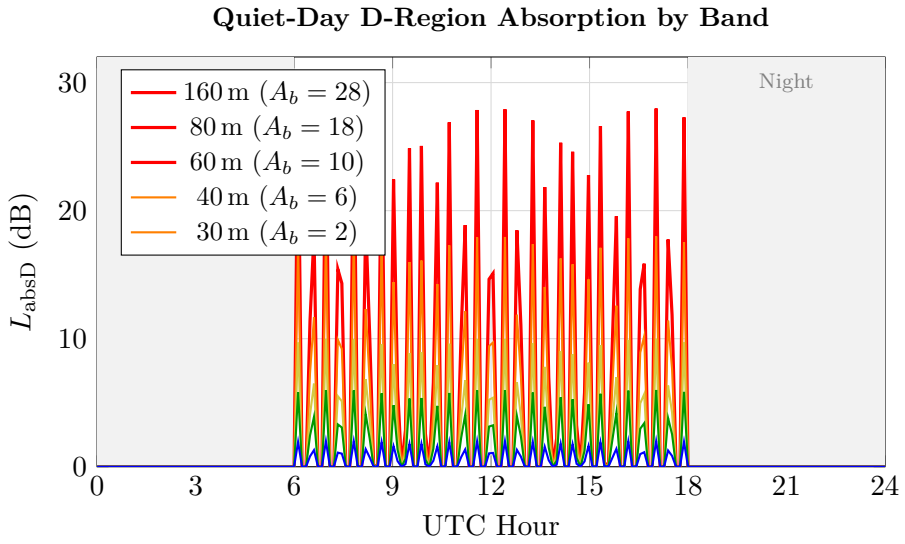


Figure 8: Quiet-day D-region absorption by band. 160 m reaches 28 dB at local noon; 30 m and above are essentially unaffected. Night absorption is zero.

## 8 Output Formatting and Alerts

The tiers and indices produced by the foregoing pipeline are surfaced in the web UI in two places: a narrative *Current Conditions* paragraph and an *Active Alerts* panel combining official SWPC notices with rule-derived ones. This section documents the assembly logic, not the copy style.

### 8.1 Current-Conditions Paragraph

The paragraph is composed in a fixed order of up to ten clauses. Any clause whose input is null or below threshold is omitted.

1. **Opener with state label and drivers.** The state label follows the five-tier $K_p$ classification used elsewhere in the app: *quiet* ($K_p < 4$), *unsettled* ($4 \le K_p < 5$), *active* ($5 \le K_p < 6$), *storm* ($6 \le K_p < 7$), *severe storm* ($K_p \ge 7$). An M- or X-class flare in progress promotes the label to at least *active* so the opener cannot read "quiet" while the D-region is being chewed through. The parenthetical driver list carries SFI, SN, $K_p$, and $A_p$ when available.

2. **Flare sentence.** Fires when the current GOES XRS class is C5 or above, with escalating language at M and X.

3. **Geomagnetic sentence.** Fires for $K_p \ge 5$ with escalating operational language (minor storm → severe storm). The bare "field unsettled" line for $K_p \in [4, 5)$ is suppressed: the opener already carries that word, so a dedicated sentence would be redundant.

4. **HF band sentence.** Bands are grouped by tier: excellent, good, marginal, weak, closed. In the *degenerate* case where every HF band sits in one tier — common in uniformly poor or uniformly good conditions — the sentence reads "HF *tier*: 160 m, 80 m, …, 10 m." without repeating the tier word after the list. Otherwise the multi-tier form "HF: *bands tier*; *bands tier*; …" is used.

5. **Noise floor and D-region coda.** The 20 m S-unit noise floor is appended to the HF sentence. When DRAP at QTH $\ge 5$ MHz a D-region absorption clause is appended too.

6. **Kp attribution (optional).** When $4 \le K_p < 5$ and the upper HF bands (15, 12, 10 m) sit strictly below the mid HF bands (20, 17 m) in tier rank, the clause "Upper HF depressed by elevated Kp." is appended to the HF sentence. For $K_p \ge 5$ the explicit geomagnetic sentence already covers this, so the attribution is skipped to avoid duplication.

7. **Gray-line enhancement (optional).** Evaluates $B_{\mathrm{GL}}(3.5\,\mathrm{MHz})$ at the operator's QTH using equation (26). When the bonus is $\ge 2$ dB — i.e. the terminator is within $\sim 4^\circ$ of the QTH meridian — a standalone sentence announces the window. The threshold corresponds to roughly the middle of the $\sim$30 min terminator pass.

8. **VHF sentence.** Picks one of four forms by priority: (i) sporadic-E when any VHF band is tiered *good* via Es; (ii) aurora when OVATION HP $\ge 50$ GW; (iii) tropospheric ducting when $\Delta N \le -100$ N-units; (iv) tropospheric enhancement when $-100 < \Delta N \le -50$; else (v) a default "VHF/UHF closed" line. $\Delta N$ is derived from the nearest University of Wyoming radiosonde via the refractivity formula

$$N = \frac{77.6}{T}\left(P + \frac{4810\,e}{T}\right)$$

   evaluated at the surface and at surface + 1 km altitude.

9. **Trending clause.** Projected transitions at the +3, +6, and +12 h horizons (first tier change per band, equation (27) evaluated at each checkpoint) are clustered by direction, destination tier, time-of-day, and storm hint. Adjacent bands that share all four keys merge into a single phrase: a two-band cluster uses a comma ("160 m, 80 m drop to closed by 11:00 UTC"), a three-or-more-band run uses an en-dash range ("15–10 m drop to poor by 14:00 UTC"), and verbs pluralise in the cluster form.

10. **72-hour outlook and 27-day coda.** Either the SWPC 3-day probability row with operational implication, or the default "Quiet conditions expected over the next 72 hours." The 27-day ISES overlay appends a second sentence when $A_p \geq 25$ or when the forecast SFI swings by $\geq 25$ relative to today.

### 8.2 Active Alerts Panel

The alerts panel combines two rendering pipelines into one severity-sorted list.

**Official SWPC feed.** A polling fetch of `products/alerts.json` emits up to four recent items. Each item's severity level is derived from its `product_id` by regex: matches on `ALERT` or `WARNING` render as *alert*, `WATCH` as *watch*, `SUMMARY` or `FORECAST` as *info*; the fallback is *warn*.

**Rule-derived (soft) alerts.** Six rules run on every refresh against the same data bundle that feeds the paragraph ($K_p$, $B_z$, $D_{\mathrm{st}}$, aurora HP, DRAP, GOES X-ray). Each rule is *graded* and short-circuits at the highest matching tier, so $K_p = 9$ does not simultaneously fire G5, G4, G3, G2, and G1. Thresholds reuse the constants documented in Sections 3–5; no new magic numbers are introduced.

Table 5: Soft-alert rule set. Severity maps to the same *info / warn / watch / alert* levels used by the SWPC renderer; *alert* ranks highest.

| **Trigger** | **Threshold** | **Level** | **Label** |
|---|---|---|---|
| X-ray flare | class $\geq$ X | alert | FLARE |
| | class $\geq$ M5 | alert | FLARE |
| | class $\in$ M1–M4.9 | watch | FLARE |
| Geomagnetic $K_p$ | $K_p \geq 9$ | alert | G5 |
| | $K_p \geq 8$ | alert | G4 |
| | $K_p \geq 7$ | alert | G3 |
| | $K_p \geq 6$ | alert | G2 |
| | $K_p \geq 5$ | watch | G1 |
| IMF $B_z$ southward | $B_z \leq -10\,\mathrm{nT}$ | alert | BZ SOUTH |
| | $B_z \leq -5\,\mathrm{nT}$ | watch | BZ SOUTH |
| Ring current $D_{\mathrm{st}}$ | $D_{\mathrm{st}} \leq -150\,\mathrm{nT}$ | alert | DST |
| | $D_{\mathrm{st}} \leq -100\,\mathrm{nT}$ | alert | DST |
| | $D_{\mathrm{st}} \leq -50\,\mathrm{nT}$ | watch | DST |
| Aurora HP | HP $\geq 100\,\mathrm{GW}$ | watch | AURORA |
| | HP $\geq 50\,\mathrm{GW}$ | info | AURORA |
| D-region absorption at QTH | DRAP $\geq 10\,\mathrm{MHz}$ | alert | ABSORPTION |
| | DRAP $\geq 5\,\mathrm{MHz}$ | watch | ABSORPTION |

Soft alerts render alongside SWPC notices rather than only when the official feed is empty: the derived context — southward $B_z$, falling $D_{\mathrm{st}}$, DRAP blanketing QTH — is material information SWPC does not publish until formal watch or warning bulletins are issued, which may lag the underlying event by several hours.

# 9 Known Limitations and Future Work

1. **Validation harness needs 2–4 weeks for meaningful skill scores.** Until sufficient WSPR-scored samples accumulate, the bias correction defaults to zero and sigma to the base 8 dB.

2. **Antenna pattern is simplified.** Elevation-dependent gain is now modelled, but the patterns are piecewise-linear approximations of typical installations, not full NEC-derived radiation plots. Real patterns vary with ground conductivity, height in wavelengths, and nearby structures.

3. **NVIS model uses foF2 directly.** For paths $< 500$ km the model substitutes GIRO foF2 as the effective MUF. A more accurate NVIS model would account for layer height and off-vertical angles up to $\sim 70\,^\circ$.

4. **No receive-side directional noise rejection.** A Yagi pointed at the target rejects off-axis noise by its front-to-back ratio (5 dB–15 dB). This effective SNR improvement is not yet modelled.

5. **Equatorial anomaly not modelled.** The EIA fountain effect produces +40–60% higher foF2 at $|\phi| \in [5^\circ, 20^\circ]$. Our climatology uses a mild linear latitude factor that misses this bump.

6. **Prediction skill not yet quantified.** The tiers produced by this pipeline are physically grounded, but their agreement with observed reality has not been measured in volume. The built-in self-calibration harness (Section 6) will tighten per-band bias and sigma as the user accumulates scored samples; until then, the verdicts remain *plausible* rather than *validated*. A companion benchmark workspace outside the ionocast repo collects aligned snapshots of ionocast's predictions, the N0NBH HamQSL tier feed, and WSPR per-band spot-density ground truth so that agreement matrices, per-band error histograms, and Brier scores on the tier probability surface can be computed once a few weeks of data have accumulated.

# A Default Settings

Table 6: Default operator settings.

| **Parameter** | **Default Value** | **Notes** |
|---|---|---|
| Transmit power $P_{\text{tx}}$ | 50 dBm (100 W) | Typical HF transceiver |
| Antenna gain $G_{\text{ant}}$ | +5 dBi | Installed dipole w/ ground reflection |
| Mode | SSB | $S_{\text{req}} = +10$ dB |
| Noise environment | Suburban | $F_a = +15$ dB |
| Reference bandwidth | 2.5 kHz | SSB passband |
| Spread $\sigma$ | 8 dB | ITU-R P.533 typical-day |
| Ensemble weights | 0.7 / 0.3 | Physics / heuristic |
| Tier width | 11 dB | For bias $\leftrightarrow$ dB conversion |
| kc2g freshness gate | 30 min | Stale data discarded |
| Hop distance | 4000 km | Assumes $h_F = 300$ km |

# B Noise Floor Table

Table 7: NOISE_FLOOR_DBM table with ITU-R P.372 cross-reference. Values at 2.5 kHz reference bandwidth. Man-made noise offset $F_a$ is added to $N_{\text{base}}$ for each environment.

| **Band** | $f$ (MHz) | $N_{\text{base}}$ (dBm) | Rural (dBm) | Suburban (dBm) | Urban (dBm) |
|---|---|---|---|---|---|
| 160 m | 1.8 | -110 | -110 | -95 | -85 |
| 80 m | 3.5 | -115 | -115 | -100 | -90 |
| 60 m | 5.3 | -118 | -118 | -103 | -93 |
| 40 m | 7.0 | -122 | -122 | -107 | -97 |
| 30 m | 10.1 | -125 | -125 | -110 | -100 |
| 20 m | 14.1 | -128 | -128 | -113 | -103 |
| 17 m | 18.1 | -131 | -131 | -116 | -106 |
| 15 m | 21.1 | -132 | -132 | -117 | -107 |
| 12 m | 24.9 | -133 | -133 | -118 | -108 |
| 10 m | 28.1 | -134 | -134 | -119 | -109 |

The P.372 external noise figure $F_a$ for galactic noise is incorporated into $N_{\text{base}}$. The suburban and urban columns show the man-made floor $N_{\text{mm}} = N_{\text{base}} + F_a$ that dominates the power sum in most residential environments.

## References

## References

[1] ITU-R Recommendation P.533-14, *Method for the Prediction of the Performance of HF Circuits*, International Telecommunication Union, Geneva, 2019.

[2] ITU-R Recommendation P.372-14, *Radio Noise*, International Telecommunication Union, Geneva, 2019.

[3] ITU-R Recommendation P.1239-3, *ITU-R Reference Ionospheric Characteristics*, International Telecommunication Union, Geneva, 2015.

[4] ITU-R Recommendation P.525, *Calculation of Free-Space Attenuation*, International Telecommunication Union, Geneva.

[5] ITU-R Recommendation P.534, *Method for Calculating Sporadic-E Field Strength*, International Telecommunication Union, Geneva.

[6] ITU-R Recommendation P.842, *Computation of Reliability and Compatibility of HF Radio Systems*, International Telecommunication Union, Geneva.

[7] ARRL, *The ARRL Antenna Book* and *The ARRL Handbook for Radio Communications*, 2023 editions, American Radio Relay League, Newington, CT.

[8] C. Luetzelschwab (K9LA), "Quiet-day D-region absorption tables," personal communication and online articles, https://www.k9la.us/.

[9] J. H. Taylor (K1JT), "WSJT-X: Digital Modes for Weak Signal Communications," https://wsjt.sourceforge.io/wsjtx.html.

[10] T. J. Fuller-Rowell, M. V. Codrescu, R. G. Roble, and A. D. Richmond, "How does the thermosphere and ionosphere react to a geomagnetic storm?" in *Magnetic Storms*, Geophysical Monograph 98, pp. 203–225, American Geophysical Union, 1994.

[11] M. Mendillo, "Storms in the ionosphere: Patterns and processes for total electron content," *Reviews of Geophysics*, vol. 44, RG4001, 2006. DOI: 10.1029/2005RG000193.

[12] G. W. Prölss, "Ionospheric F-region storms," in *Handbook of Atmospheric Electrodynamics*, vol. 2, pp. 195–248, CRC Press, 1995.